

Mechanisms of nitrous oxide emissions in biochar treated plots

Master Thesis

submitted by

Jutta Grabenhofer

0940317

Supervision:

Univ. Prof., Dr. phil. Sophie Zechmeister-Boltenstern (BOKU, AUT)

Tim Clough, PhD (Lincoln University, NZ)



Vienna, September 2016

Acknowledgements

Special thanks go to Rebecca Hood-Nowotny (Austrian Institute of Technology) and Tim Clough (Lincoln University, NZ), who supervised me during the past months and had a big contribution in the research activities for this thesis.

Moreover, this research was only possible due to the excellent contribution of colleagues from the FAO/IAEA Joint Division.

All my gratitude goes to my family, for years of support and guidance.

Affidavit

I hereby declare that I am the sole author of this work. No assistance other than that which is permitted has been used. Ideas and quotes taken directly or indirectly from other sources are identified as such. This written work has not yet been submitted in any part.

Vienna, September 2016

Abstract

Biochar amendment of soil has been found to have positive effects on soil physical properties and it has phenomenal C-sequestration potential. Moreover, there is evidence that it impacts the N-cycle as it changes the nitrification and denitrification dynamics in soil. These changes in turn could affect the N₂O emissions. This is particularly important as N₂O is a climate relevant greenhouse gas with approximately 300-times the global warming potential of CO₂. Understanding the dynamics of N₂O production in soil and its adaptations due to the incorporation of biochar is crucial if we are to effectively manage this important climate combating resource. Stable isotope techniques using ¹⁵N and ¹⁸O were recently found to be essential in determining these N₂O dynamics and new laser based cavity ring down spectrometric (CRDS) methods have become available, which allow us to investigate the N₂O sources in a laboratory setting. This enables us to systematically investigate the different processes behind N₂O production. Therefore, in a laboratory based experiment we investigated the sources of N₂O emissions using soils from a field experiment where biochar had been incorporated five years prior to the laboratory experiment. Soil samples of different biochar treatments (24 t ha⁻¹ and 72 t ha⁻¹ biochar addition with 120 kg ha⁻¹ N-fertilizer) were analysed by stable isotope analysis. Isotope ratio mass spectrometry (IRMS) was performed on ¹⁵N labelled soil samples and N₂O fluxes were measured with a LGR (CRDS) Isotopic N₂O Analyzer. In this study, there were no significant differences in the nitrous oxide fluxes, nitrification rates and N turnover rates between the biochar treatments and our control plots. This suggests that five years after biochar application, there was no significant effect of biochar on the mechanisms underpinning N₂O emissions in this arable soil. Moreover, gross nitrification rates observed were higher than net nitrification rates suggesting large dinitrogen losses from the system. However, the proportion of N₂O derived from denitrification was found to be substantially lower than the N₂O emissions from nitrification, which could imply efficient denitrification under aerobic soil conditions. These results again highlight the importance of studying all possible N loss mechanisms to gain a full understanding of N dynamics under new management systems. Due to the very limited amount of long-term studies on biochar correlation to N₂O emissions, more research is needed on its effects.

ABBREVIATIONS

AIT	Austrian Institute of Technology
BC1N	Biochar plot with 30kg ha ⁻¹ Biochar
BC3N	Biochar plot with 90 kg ha ⁻¹ Biochar
C	Carbon
CH ₄	Methane
CO ₂	Carbon dioxide
DNRA	Dissimilatory nitrate reduction to ammonium
FAO	Food and Agriculture Organisation
HCl	Hydrochloric acid
IAEA	International Atomic Energy Agency
IRMS	Isotope ratio mass spectrometry
K	Hydraulic conductivity
K ₂ SO ₄	Potassium sulfate
KCl	Potassium chloride
KHSO ₄	Potassium hydrogen sulfate
KNO ₃	Potassium nitrate
LGR	Los Gatos Research
MgO	Magnesium oxide
N	Nitrogen
N ₂	Dinitrogen
N ₂	Dinitrogen
N ₂ O	Nitrous oxide
NH ₂ OH	Hydroxylamine
NH ₃	Ammonia
NH ₄	Ammonium
NH ₄ Cl	Ammonium chloride
NO	Nitric oxide
NO ₂	Nitrite
NO ₃	Nitrate
N _{org}	Organic nitrogen
NPK	Non-biochar control plot
Ppbv	Parts per million (by volume)
Ppm	Parts per million
SD	Standard deviation
VCl ₃	Vanadium trichloride
WFPS	Water-filled pore space
XS	Excess

LIST OF FIGURES

FIGURE 1. GLOBAL N-CYCLE (IN TG/YEAR)	2
FIGURE 2. SCHEME OF PREDOMINANT MICROBIAL PATHWAYS OF N ₂ O PRODUCTION	5
FIGURE 3. PATHWAYS OF N ₂ O EMISSIONS	8
FIGURE 4. NITRATE DETERMINATION WITH THE ENSPIRE MICROTITER PLATE READER	20
FIGURE 5. PREPARATION FOR THE MICRO DIFFUSION AND IRMS	21
FIGURE 6. LGR MEASUREMENT SYSTEM FOR N ₂ O DETERMINATION	24
FIGURE 7. CONCENTRATION OF AMMONIUM IN SOILS PLOTTED AGAINST TIME	28
FIGURE 8. CONCENTRATION OF NITRATE IN SOILS PLOTTED AGAINST TIME	29
FIGURE 9. N ₂ O FLUX DATA	31
FIGURE 10. PROPORTION OF N ₂ O EMISSIONS FROM NO ₃ AND ALL OTHER POOLS	32
FIGURE 11. NET NITRIFICATION RATES OF NO ₃ AND NH ₄ SOURCES	33
FIGURE 12. GROSS NITRIFICATION RATES PER HOUR	35

LIST OF TABLES

TABLE 1: PLOT TREATMENTS	17
TABLE 2. INORGANIC N CONCENTRATIONS IN SOILS	27
TABLE 3. GAS EMISSIONS FROM N ₂ O ANALYSIS	30
TABLE 4. NET NITRIFICATION RATES	32
TABLE 5. GROSS NITRIFICATION RATES	34
TABLE 6. PROBABILITY OF TREATMENT EFFECTS	38

LIST OF EQUATIONS

EQUATION 1. ACTUAL N- CONCENTRATION X_{NH_4} FOR IRMS OF AMMONIUM SAMPLES	20
EQUATION 2. ACTUAL N- CONCENTRATION X_{NO_3} FOR IRMS OF NITRATE SAMPLES	20
EQUATION 3. NO ₃ DETERMINATION BY ATOMIC FRACTION	22
EQUATION 4: PERCENTAGE N ₂ O FROM THE NITRATE POOL	22
EQUATION 5: ISOTOPE RATIO VS. AIR-NITROGEN	24
EQUATION 6: ISOTOPIC TWO-POOL-SOURCE MIXING MODEL	25

TABLE OF CONTENT

1. INTRODUCTION	1
1.1. THE NITROGEN-CYCLE	2
1.2. RELEVANT PATHWAYS OF N ₂ O	4
1.2.1. NITRIFICATION	5
1.2.2. DENITRIFICATION	6
1.3. STABLE ISOTOPES	8
1.4. BIOCHAR IN ECOLOGICAL STUDIES	9
1.4.1. DEFINITION	10
1.4.2. STRUCTURAL PROPERTIES	10
1.4.3. BIOCHAR-INDUCED PHYSICAL ADAPTATIONS IN SOIL	12
1.5. LINKING BIOCHAR TO N ₂ O EMISSIONS	14
2. METHODS	16
2.1. EXPERIMENTAL SITE	16
2.2. SOIL SAMPLING AND EXPERIMENTAL DESIGN	17
2.3. INORGANIC N DETERMINATION	18
2.4. MICRO DIFFUSION AND ISOTOPE RATIO MASS SPECTROMETRY	20
2.5. N ₂ O SAMPLING	23
2.6. GROSS VS. NET NITRIFICATION	25
2.7. STATISTICAL ANALYSIS	26
3. RESULTS	26
3.1. INORGANIC N DETERMINATION	27
3.2. N ₂ O GASEOUS ANALYSIS	29
3.3. NITRIFICATION RATES	32
4. DISCUSSION	35
4.1. INORGANIC N DETERMINATION	35
4.2. N ₂ O GASEOUS ANALYSIS	36
4.3. NITRIFICATION RATES	37
4.4. BIOCHAR VS. NON-BIOCHAR TREATMENT	38
5. CONCLUSION AND OUTLOOK	38
6. REFERENCES	40

1. Introduction

While carbon dioxide (CO₂) is the most known and researched greenhouse gas, methane (CH₄) and nitrous oxide (N₂O) also contribute to global warming having 25 times (CH₄) and 298 times (N₂O) of the CO₂ equivalent mass (Forster et al., 2007; Ravishankara et al., 2009).

Studies suggest, that N₂O emissions from soil are affected by biomass application. Soil-physical properties such as water retentions and soil aggregation (Quin et al., 2014), soil chemical properties (e.g. pH, N_{org}, minimum N, dissolved organic C, etc.) and soil biological properties (e.g. microbial biomass content, N cycling enzymes, macro fauna, etc.) might be influenced with additional carbon incorporation (Harter et al., 2014). Biochar amendment in soil as source of carbon has been found to have positive effects on soil physical properties and the C-sequestration potential. Moreover, it might impact the N-cycle as it changes the nitrification and denitrification dynamics in soil (Harter et al., 2014).

Next to autotrophic nitrification and heterotrophic denitrification, several other mechanisms were found that contribute to the production and consumption of N₂O from soil. These include nitrifier denitrification, heterotrophic nitrification, co-denitrification and dissimilatory NO₃⁻ reduction (Hu et al., 2015). To differentiate between nitrification and denitrification processes in soil, ¹⁵N stable isotope enrichment studies can be used (Baggs, 2008).

The aim of this study is to determine the mechanisms of nitrous oxide emissions in biochar amended soils by using stable isotope analysis of ¹⁵N. The main focus of this research is heterotrophic denitrification as well as nitrifier denitrification as main sources of N₂O production in soils (Wrage et al., 2005).

We identified the main research question of the thesis as following:

Does biochar amendment in arable soil change N₂O production mechanisms by shifting heterotrophic nitrification to nitrifier-denitrification?

We posited two hypotheses to tackle the research question.

Hypothesis I: *Adding biochar results in a shift of N₂O production from heterotrophic nitrification to nitrifier-denitrification.*

Hypothesis II: N_2O emissions are derived from ammonia oxidation rather than from nitrifier denitrification.

In the first part of the thesis there is a theoretical overview of the nitrogen cycle and the predominant mechanisms behind the formation of N_2O emissions. Furthermore, the methods and applications of stable isotope tracers are discussed. Due to the crucial impact of organic carbon on N_2O emissions, biochar as soil amendment is discussed as regulator for nitrification and denitrification processes. Moreover, the methodology behind our research is explained. Additionally, the results are presented and discussed.

1.1.□ The Nitrogen-Cycle

N_2O is a greenhouse gas contributing crucially to global warming as it has a global warming potential that is 298 times higher than the CO_2 equivalent mass (Forster et al., 2007). Since the Industrial Revolution, anthropogenic sources of N_2O have increased substantially. Harter et al. (2014) relate this to the expansion of farming activities followed by the intensification of fertilizer use. It has been suggested that 56-70% of N_2O emissions can be traced back to agricultural emissions (Butterbach-Bahl et al., 2013). Next to anthropogenic emissions, soil and oceans are the main sources and sinks of natural N_2O emissions, which react to stratospheric NO_x causing severe environmental problems (Ravishankara et al., 2009).

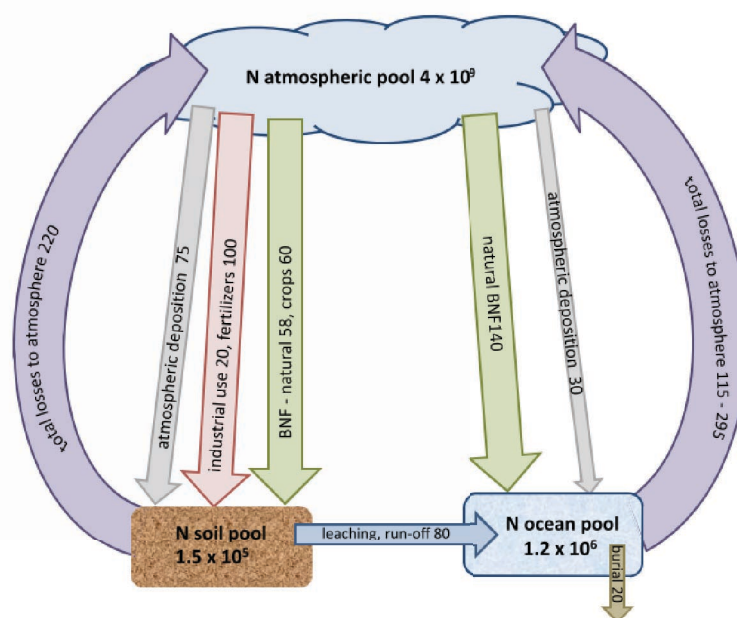


Figure 1. Global N-Cycle (in Tg/year) (source: Hirsch and Mauchline, 2015, p. 47)

Hirsch and Mauchline (2015) estimated the global atmospheric fixation of N into soil to be around 1.5×10^5 Tg each year (Figure 1). The local N-cycle and the site specific N-flux in soil is determined by its production and consumption processes (Van Zwieten, et al., 2015). The main climate related issue for soil N is the production of N₂O through key soil processes, such as denitrification and nitrification. Soil microbial activity is a key to understanding these processes. Several parameters determine the N₂O production and consumption processes such as oxygen supply and temperature (Butterbach-Bahl et al., 2013). As N₂O emissions result from various temperature dependent processes, Butterbach-Bahl et al. (2013) observed a multiplying effect of temperature on N₂O emissions resulting in a greater greenhouse gas potential of N₂O compared to CO₂.

Local N₂O emissions from soil are characterized by hot-spots of N₂O production. These are spatial temporal variabilities in N₂O fluxes from soil arising as a result of leaching, erosion, fertilizer application and ruminant grazing (Butterbach-Bahl et al., 2013).

There are several predominant factors regulating the N₂O production and consumption in soil (Dalal et al., 2003):

- **Moisture and aeration of soil:** N₂O production from nitrification in soil is low if water-filled pore space (WFPS) accounts for up to 40 % of the total pore space. With increasing water content aeration becomes poor and denitrifiers dominate N₂O formation. Denitrification has been found to be at an optimum between 70-80% WFPS (Butterbach-Bahl et al., 2013).
- **Temperature:** Nitrification and denitrification rates are affected by temperature. Both processes increase with rising temperatures. In particular, denitrification is especially susceptible to temperature changes (Dalal et al., 2003).
- **Organic matter:** The incorporation of additional organic matter was found to increase N₂O production in soils, especially due to higher denitrification rates (Dalal et al., 2003).
- **Soil nitrogen and N-fertilizer:** A higher NO₃⁻ content in soil favours denitrification and blocks the transformation from N₂O to N₂ to a certain

extent. Under aerobic conditions there is a clear relationship between NH_4^+ present in the soil and the production of N_2O . Hence, nitrification enhances N_2O formation (Dalal et al., 2003).

- **pH and salinity of soil:** Nitrification and denitrification are favoured at pH levels of 7 to 8. It was found that salinity may enhance N_2O emissions from nitrification (Dalal et al., 2003).
- **Other nutrients:** Other nutrients might limit the capability of using $\text{NH}_4\text{-N}$ and $\text{NO}_3\text{-N}$. Studies on phosphorous showed increasing N_2O emissions with phosphorous being a limiting factor. This implies the important interaction of N with other nutrients for plant growth (Dalal et al., 2003).

Some studies have observed that up to 95% of the temporal variation in N_2O emissions can be explained by changes in moisture content and temperature alone (Butterbach-Bahl et al., 2013).

1.2. Relevant pathways of N_2O

Robertson and Groffman (2015) identified the main processes affecting the N cycle in soil as N-mineralization, N-immobilization, nitrification and denitrification. After briefly introducing mineralization and immobilization, this paragraph will give an overview about the most important characteristics of nitrification and denitrification as identified as most important paths of N_2O in our study.

During mineralization, organic N is transformed to inorganic N. This is produced as a by-product of the consumption of soil organic matter including detritus by microorganisms. NH_4^+ is directly produced by mineralization. Immobilization on the other hand is the assimilation of inorganic N by microorganisms. This occurs if there is an insufficient supply of organic N from soil organic matter and microbial demand for nitrogen. Both processes can occur at the same time as different microorganisms are tackling different elements of soil organic matter breakdown (Robertson and Groffman, 2015). In general, if decomposing processes are low, mineralization is low as well. In such a scenario, immobilization would be high as a result of a high NH_4^+

uptake. As a result, nitrification rates would generally be low (Robertson and Groffman, 2015).

Nitrification and denitrification are determined by the level of O_2 in soil and the availability of inorganic N – NO_3^- and NH_4^+ (Robertson and Groffman, 2015). The two paths can further be split into nitrite oxidation, heterotrophic denitrification, ammonia oxidation, nitrifier denitrification, anaerobic ammonium oxidation and nitrate ammonification (Hu et al., 2015). According to Hu et al. (2015) the critical processes in the N_2O cycle in soil are heterotrophic denitrification and the pathways of nitrification including ammonia oxidation and nitrifier denitrification (figure 2).

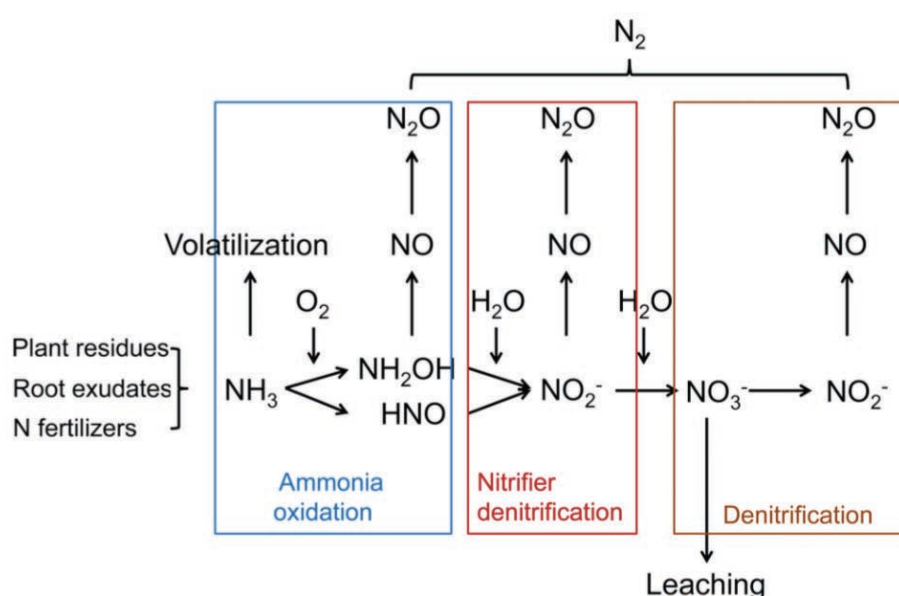


Figure 2. Scheme of predominant microbial pathways of N_2O production (source: Hu et al., 2015, p.738)

1.2.1. □ Nitrification

Nitrification is favoured by aerobic soil conditions, optimum soil temperatures, pH 6-7 and high NH_4^+ concentrations (Case et al., 2015). Autotrophic nitrification is recognized as being a dominant process of nitrification in most systems although heterotrophic microbes and archaea have also been found to be capable of the transformation (Robertson and Groffman, 2015).



Ammonia oxidation is the limiting step in N₂O production. Some studies suggest that it contributes up to 80% to N₂O emissions from soil (Hu et al., 2015). In contrast, there are a number of studies suggesting a rather large contribution of nitrifier denitrification to overall N₂O production (Kool et al., 2010). In particular, Kool et al. (2010) state, that many studies overestimate the role of ammonia oxidation by ammonia-oxidizing bacteria if nitrifier denitrification is not taken into account. In their study, nitrifier denitrification had a severe impact on N₂O emissions under certain moisture conditions.

Nitrifier denitrification is classified as a special form of nitrification mediated through autotrophic nitrifiers (Kool et al., 2010). It can be the source of NO_x and N₂O under oxygen limited conditions (Robertson and Groffman, 2015). Different to ammonia oxidation, it is characterized by a prior oxidation of ammonia to nitrite. After this step, nitrite is reduced from NO to N₂O (Hu et al., 2015).



Several ammonia-oxidizing bacteria are able to denitrify NO₂⁻ to N₂O. Not all of them can be found in soil. In this medium *Nitrosospira spp.* are the most common ones (Kool et al., 2010).

Although the term nitrifier denitrification is used in various ways in literature, in this study we use the definition of Robertson and Groffman (2015) that classifies nitrifier denitrification as N₂O and NO_x formation via nitrifiers when O₂ levels are low or produced as a by-product of other processes.

1.2.2. Denitrification

Although nitrous oxide emission from nitrifier denitrification and ammonia oxidation have been shown to be important processes in some soils rather different results were found by Case et al. (2015). In their experimental setup denitrification accounted for the majority of N₂O emissions from arable soil. This highlights the contextual nature of the predominant sources of nitrous oxide emission.

During denitrification, NO_3^- is reduced to $\text{N}_{2\text{gas}}$, NO , N_2O and N_2 . In oxygen depleted environments such as flooded soil or soil with high microbial activity, O_2 is usually the limiting factor for denitrifiers, and they use NO_3^- as electron acceptor (Robertson and Groffman, 2015). Denitrification is fostered by decreasing pH values within soil and an increasing concentration of NO_3^- . Furthermore, the carbon concentration and an increase in WFPS determine the denitrification potential (Case et al., 2015). Denitrification is a crucial mechanism for the global N-cycle as it returns N to the atmosphere as N_2 (Robertson and Groffman, 2015).

The process of heterotrophic denitrification is dominant in oxygen-limited environments with the consumption of carbon as energy supply. There are four enzymes involved in the process. Nitrate reductase (Nar) converting NO_3^- to NO_2^- , nitrite reductase (Nir) facilitating the conversion of NO from NO_2^- , nitric oxide reductase (Nor) converting NO to N_2O and N_2O reductase (Nos) converting N_2O to N_2 (Robertson and Groffman, 2007).



N_2O is not always subsequently converted to N_2 . As product of heterotrophic denitrification it can become the end product of the process chain. N_2O can be produced via heterotrophic denitrification in soils with low pH and low oxygen levels. Consumption of N_2O appears to be predominant in grassland and forest with high carbon availability and low concentration of mineralized nitrogen, thus heterotrophic denitrification can either lead to soil becoming a N_2O sink or source (Hu et al., 2015).

Van Zwieten et al. (2015) reiterate, that all described processes are highly dependent on soil physical characteristics such as water content, temperature, pH and texture as well as soil biological parameters (e.g. microbial activities). The correlation between pH and N_2O as well as O_2 levels and N_2O is shown in figure 3. With an increasing oxygen level the relative contribution of N_2O production shifts from heterotrophic denitrification to ammonia oxidation. Regarding the dependence of N_2O production on the pH value, nitrifier denitrification seems to increase with higher pH while ammonia oxidation and heterotrophic denitrification decrease respectively. As incorporation of organic carbon (i.e. biochar) can lead to a local increase in pH, there might be a tendency to an alteration in nitrifier denitrification in treated soils.

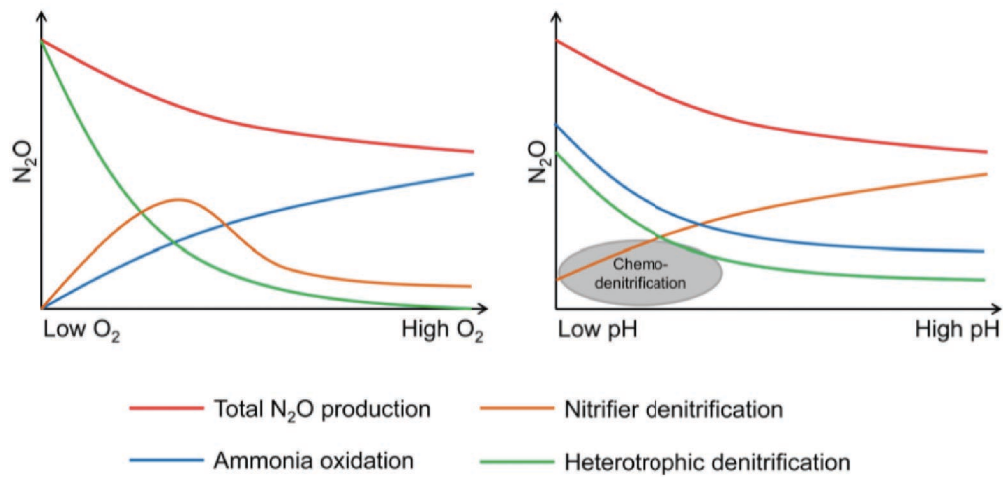


Figure 3. Pathways of N_2O emissions: Relative contribution of ammonia oxidation, nitrifier denitrification and heterotrophic denitrification to N_2O production along the O_2 and soil pH gradients (source: Hu et al., 2015, p. 734)

Several tools are used to quantify soil processes. For observing differences in nitrification and denitrification Butterbach-Bahl et al. (2013) recognize three methods: (i) inhibitor techniques, (ii) molecular techniques and (iii) stable isotope techniques. For this study (iii) a stable isotope technique was applied.

In this study (iii) stable isotope technique of the ^{15}N isotope was used to identify characteristics of relevant mechanisms of N_2O emissions. The next paragraph will give an overview about characteristics of stable isotopes in general and explain how recent N_2O studies use stable isotopes for their purpose.

1.3. □ Stable Isotopes

Stable isotopes can be extremely useful in tracing the processes in the nitrogen cycle in soils. Isotopes can be differentiated by the number of neutrons while having an equal number of electrons and protons of the original atom. Isotopes can appear in an unstable or stable state. Unstable isotopes are characterized by a radioactive decay, stable isotopes are energetically stable, which is one of the reasons why they are frequently used in ecological studies (Sulzman, 2007).

E. Sulzman (2007) distinguished several properties of stable isotopes which were identified to be crucial for the use in ecological studies:

- Small atomic mass
- Atomic differences between abundant and rare isotopes have to be large
- An isotope has to have two or more oxidation states

Ecological studies have been using stable isotope techniques to determine the sources of N_2O production from nitrifier denitrification and denitrifiers. These methods are based on a non-invasive measurement of changes in the composition of stable isotopologue and isotopomer (Snider, et al., 2009).

The stable isotope signature of the isotopomer of N_2O is characterized by an α -position located in the centre of the N_2O molecule and a peripheral β -position (Sielhorst, 2014). These changes can be measured and used to trace changes in isotopic composition and the N_2O molecule consists of $\delta^{15}\text{N}$ and $\delta^{18}\text{O}$.

For this study, the natural differences in abundance of the isotopes is negligible as a highly labelled ^{15}N -isotope is used as tracer substance and its signal swamps any natural differences seen in non-tracer studies.

In N_2O studies, ^{15}N is frequently used to differentiate nitrification and denitrification processes from one another by applying fertilizer that is ^{15}N -labelled (Baggs, 2008). By labelling soil cores with a ^{15}N enriched solution, N_2O fluxes can be measured and traced to NH_4^+ and NO_3^- pools of the mechanisms behind N_2O production and consumption. In stable isotope enrichment studies denitrification can be traced back to the application of $^{15}\text{N}\text{-NO}_3$. Nitrification on the other hand is related to the use of $^{15}\text{N}\text{-NH}_4$ (Baggs, 2008). Baggs (2008) suggests two ways of applying enriched ^{15}N to samples. This can be done either by using $^{14}\text{NH}^{15}\text{NO}$ or $^{15}\text{NH}^{15}\text{NO}$. In common enrichment studies, ^{15}N is enriched at less than 1 atom % excess (XS). This is due to the characteristic of ^{15}N isotopes to have an isotopic fractionation that does not depend on its enrichment (Baggs, 2008).

1.4. Biochar in ecological studies

Biochar can be used in several environmental disciplines to increase soil stability, fertility and improve hydraulic properties of soil (Masiello et al., 2015). Recent studies suggest that biochar might also be able to mitigate climate relevant greenhouse gasses such as N_2O (Harter et al., 2014).

This following paragraph provides a definition of biochar and gives an overview of important mechanisms influencing and influenced by biochar properties.

1.4.1. Definition

Due to common misunderstandings of the term biochar it is crucial to distinguish between the three solid carbonaceous materials that can be derived from pyrolysis (i) char, (ii) charcoal and (iii) biochar.

While (i) char is a flammable material derived as residue of natural fires, (ii) charcoal is artificially produced from animal and vegetable matter during the pyrolysis process in a kiln. In comparison to charcoal, (iii) biochar is specifically developed for the application on soil to foster soil quality and increase agricultural yields (Brown et al., 2015, p.39). What all three processes have in common is their production technology, known as pyrolysis. It is a technology, which produces stable carbon rich matter (Bridgewater & Peacocke, 2000).

1.4.2. Structural Properties

The final characteristics of biochar and its interactions with soil are highly dependent on the feedstock used, pyrolysis process and any treatment temperature. Parameters such as heating rate, reaction pressure, residence time of the reaction and the vessel dimensions (Chia et al., 2015), all have important roles during the pyrolysis process as well. While the moisture in feedstock is lost at relatively low temperatures ($\sim 120^{\circ}\text{C}$), higher temperatures ($220\text{--}400^{\circ}\text{C}$) are needed to decompose cellulose and hemicellulose (Chia et al., 2015). In particular, it is these high temperature treatments –which need to be adapted to feedstock – as it is known that temperature has the most influence on the structure of the end product, due to rather large physical changes during the manufacturing process (Chia et al., 2015) such as changes in the structure of aromatic carbon within biochar (Keiluweit et al., 2010). According to Keiluweit et al. (2010), the material transforms towards a more crystalline structure at higher treatment temperatures. The carbon structure at around 400°C can be observed as highly disordered (amorphous). It develops towards more uniform plates of turbostratic aromatic carbon from around 800°C onwards reaching a graphitic

structure at approximately 3500°C (Keiluweit et al., 2010). During the process of biochar production temperatures are usually chosen below 600°C (Chia et al., 2015). For example, Kinney et al. (2012) observed the correlation between biochar production temperatures and field capacity in soil. The results suggest, that field capacity is highest for biochar produced at temperatures between 400°C and 600°C, with an optimum at 500°C or above. This factor was strongly dependent on feedstock. While corn stover produced above 300°C had an overall better effect on field capacity, apple wood and magnolia leaf showed little differences at production temperatures around 500°C-600°C.

Production temperature may also affect the relative pore size distribution of biochar (Chia et al., 2015; Gray et al., 2014). With higher temperature, more pores develop – especially pores smaller than 2 nm that are mainly responsible for the enlargement of surface areas of the biochar. This positive correlation between biochar production temperature and surface area occurs due to chemical modifications. As carbon condensates, pyrogenic nano-pores develop, increasing the surface area (Gray et al., 2014). It needs to be recognized though, that enlargement of surface area is not always beneficial. The presence of meso- and macro pores is crucial for water retention. Water might be retained inside biochar pores and stored between biochar particles due to capillary forces. This concept of inter- and intra-particle pores and will be discussed below (Masiello et al., 2015).

Another property affected by the highest treatment temperature is the density of biochar. With increasing temperatures, solid density increases with an inverse effect on bulk density. It can be observed, that solid densities for biochar -1.5-2.0 Mg/m³ are lower than the ones for charcoal - ~2 Mg/m³ (Jankowska et al., 1991). This effect might be correlated to surface area and porosity of biochar. Gray et al. (2014) note, that biochar with higher porosity has lower bulk density.

Moreover, biochar has an aliphatic surface. This characteristic decreases at higher pyrolysis temperatures but according to a study by Gray et al. (2014) never completely disappears. Aliphatic compounds influence biochar hydrophobicity as they foster negative capillary forces within biochar particles. Hence, water uptake in pores is inhibited (Gray et al., 2014).

Research has been tackling the great variety of feedstock used for biochar production and the effects on biochar quality. Fibrous biomass consists mainly of cellulose, hemicellulose, lignin and inorganic elements nitrogen, phosphorus,

potassium and smaller amounts of sulphur, chlorine and others (Brown et al., 2015). These substances are highly affected by climate, soil type and harvest time. Furthermore, the temperature of pyrolysis is determining decomposition of the material due to the behaviour of cellulose, hemicellulose and lignin at high temperatures (Brown et al., 2015).

1.4.3. Biochar-induced physical adaptations in soil

To understand N₂O dynamics in soil it is essential to have not only an overview about soil chemical processes but also about the most important soil physical parameters, as they are closely linked to N₂O emissions from soil (Van Zwieten et al., 2015). This chapter will give an overview about important soil hydraulic properties and their correlation to soil porosity.

There are many contradicting studies about the effect of biochar on soil hydraulic processes. Most studies suggest though, that biochar amendment in soil leads to positive impacts within soils. This includes an increase in plant available water, water-holding capacity of soils and the hydraulic conductivity. The drainage effect is influenced positively for sandy and clay soils leading to faster draining clay soils and slower draining sandy soils (Barnes et al., 2014).

Porosity is not only a crucial factor within biochar itself, but it also affects the soil to which biochar is added. The intra- and inter-particle-pores concept demonstrates the interaction between soil and biochar. Intra-particle pores allow water to move within biochar particles (Masiello et al., 2015). Hence, this concept is independent from the soil type but only depends on the properties of biochar (Lua et al., 2004). Inter-particle pores refer to the interaction between soil and biochar. Soil water movement depends highly on this interaction. If biochar particles are smaller than soil particles biochar will fill up the inter-particle space and decrease the size of it. Resulting in capillary forces that might be too strong to overcome for plants and decreasing the amount of plant available water (Masiello et al., 2015).

The overall porosity of soil increases in most observed studies after biochar incorporation (Abel et al., 2013; Herath et al., 2013). Moreover, meso- and macro

pores increase. This might result from physical changes in the soil due to biochar. It is though barely recognized in literature that there could be other forces in place such as microorganisms, micro- or mesofauna or chemical processes (Masiello et al., 2015).

The effect of biochar on hydraulic conductivity (K) is so far not clearly understood. It is known as being closely related to water infiltration in soil. High infiltration rates can be of positive or negative nature. While high infiltration rates prevent soil surface run off from intense storms, it has adverse effects on nutrient up-take for plants and other chemical processes in the soil (Lim et al., 2016). Several studies indicate that K is mostly positively affected by biochar amendment in sand and clay soils (Herath et al., 2013; Barnes et al., 2014). Hence, water flow in sandy soils decreases and leads to improved water uptake. Infiltration in clay soils is improved, hence it facilitates water drainage (Sun and Lu, 2014; Herath et al., 2013). There are only few long-term studies on the effects of biochar on K. Barnes et al. (2014) suggest, that over a longer time period, the effects of biochar might change in comparison to the observed results in field and laboratory studies during a certain trial period. This results from soil changing over time in its hydrology and soil structure. K shows a negative relation to bulk density and a positive relation to soil porosity. Meaning, with greater K, bulk density of soil decreases while with altering porosity, K also increases (Barnes et al., 2014). According to Barnes et al. (2014) soil bulk density and grain size distribution are significantly affected by biochar application.

Improved water retention is related to the high porosity of biochar (up to 80 vol%) in several studies. Moreover, as biochar has a great range of pores (0.2–50 μm) plant available water storage is clearly improved. Especially sandy soils can benefit from this characteristic as its water retention capacity was observed to improve. In clay soil adverse effects of biochar were reported (Abel et al., 2013).

Although the water storage in soil is said to increase with biochar incorporation, the availability to plants needs to be studied as well. Soil water storage includes water retention and plant available water. Plant available water is defined as the range between water held in soil at field capacity and the permanent wilting point after which plants wilt (Masiello et al., 2015). This depends a lot on the size of inter- and intra-particle pores. Plants have to overcome capillary forces to access the water. Furthermore, plant growth in drought periods can substantially be increased due to

improved water retention. Both effects were observed to be fostered by biochar amendment (Laird et al., 2013).

Masiello et al. (2015) state, that most studies on physical soil parameter in relation to biochar do not take any microbiological effects into account. Especially for understanding N₂O dynamics in soil, this factor would be crucial. The importance of the adapted water content and infiltration rates as well as the porosity becomes obvious when taking into account the N₂O dynamics and the influence of O₂ and the pH value. Which greater porosity and higher water infiltration, the O₂ content within soil pores will decrease leading to anoxic conditions. This might result in a change of nitrification and denitrification dynamics.

1.5. Linking biochar to N₂O emissions

N₂O emissions in soil can be influenced by biochar incorporation in two different ways. On the one side, biochar itself can be beneficial to soil N₂O fluxes due to its chemical and physical composition. Biochar produced at high pyrolysis temperatures has a greater surface area. This characteristic increases the absorption of N₂O molecules onto the surface structure of biochar. Moreover, WFPS of biochar has a high solubility capacity for N₂O (Van Zwieten et al., 2015).

The second way biochar influences N₂O emissions is related to the adaptations that biochar fosters in soil particles. Physical and chemical changes within soil can be improved by biochar including soil water retention, alteration of plant available N and changes in porosity of soil. Increased water retention, for example, might lead to a tendency towards anaerobic production of N₂O due to denitrification as response to a lack of oxygen in soil (Van Zwieten et al., 2015).

Furthermore, Van Zwieten et al. (2015) reviewed field and incubation studies from 30 peer-reviewed articles between 2007 and 2013. The vast majority of studies observed a clear decrease of N₂O fluxes from soil after biochar amendment. N₂O fluxes in biochar amended soils depend on several factors including soil chemical parameters. Clough et al. (2013) identifies these factors as climate, soil microbial communities, soil fertility and the nitrogen availability from soil and biochar quality characteristics. The addition of biochar to soil has been proven to foster the quality of crop yields and to positively influence various soil parameters. Moreover,

biogeochemical parameters and the potential of carbon sequestration are clearly changed by biochar addition (Chan et al., 2008).

There are other factors positively affecting N₂O emissions on biochar treated soil. According to a literature review by Van Zwieten et al. (2015) the feedstock used for biochar production is a crucial parameter for N₂O emissions. It could be observed that only biochar from wood and crop material lead to a decrease in N₂O emissions. The results were not significant for all other feedstocks. Moreover, the application rate of biochar has a great influence on the effects on soil (Van Zwieten et al., 2013). It needs to be mentioned, that most studies on biochar use application rates that are far from economically feasible for farmers, hence are not reflecting real conditions (Herath et al., 2013). Another study by Cornelissen et al. (2013) observed the ability of biochar to directly sorb N₂O gas due to its changing texture according to pyrolysis temperature. Pinewood biochar produced at temperatures above 370°C was found to have the greatest sorption capacity. Especially due to soil water infiltration into biochar pores, gas sorption might be enhanced. This strengthens the importance of understanding the influence biochar might have on the link between soil hydraulic properties and N₂O emissions.

Clough et al. (2013) mention four processes in biochar amended soils that were found by several studies to reduce N₂O emissions from soil (i) as biochar has the potential to alter porosity of soil, the soil moisture content and oxygen availability are adapted. This occurs especially in clay soils (Barnes et al., 2014; Herath et al., 2013). (ii) The impact of additional carbon matter on denitrification processes which may enhance the process of denitrification to fully transfer N₂O into N₂ (Clough et al., 2013). (iii) Biochar may increase the pH value of soil (Van Zwieten et al., 2015), leading to greater N₂O reduction to N₂. (iv) N₂O production may be inhibited due to a decrease in inorganic-N, which is needed by nitrifiers and denitrifiers to produce N₂O.

It is stated in the literature, that most studies on N₂O fluxes in biochar treated soil are short-term. There is the need for long-term experiments to understand the effects of biochar on soil. The few long-term studies that have been conducted, did not show significant effects of N₂O fluxes after the initial phase post-incorporation (Clough et al., 2013). Furthermore, although great differences between field studies compared to incubation experiments have not been observed (Van Zwieten et al., 2015), it can be

stated that so far only very few studies were actually conducted as field experiments. This leaves room for improvement and further studies at a field level to determine the actual effects on soil under natural conditions.

2. Methods

We wanted to understand the impact of biochar on denitrification and nitrifier denitrification in soils which were amended with biochar five years prior to our experiments. We wanted to investigate the biochar legacy and its impact on the processes of nitrification and N₂O losses using stable isotope labelling techniques. We set up soil core experiments in the laboratory in which we added an isotope tracer and measured the rates of nitrification and traced the pathways of N₂O losses using a new method of analysis based on cavity ring down spectroscopy and Keeling plots.

This chapter aims to give an overview about the experimental site and soil sampling for the experiments. Furthermore, the experimental setup of several methods is described in detail.

2.1. Experimental site

The field site is positioned in Traismauer in Lower Austria (AUT) (48.330315, 15.739413). Traismauer is located at 197 m above sea-level in Central Europe. A temperate climate (Pannonian climate) is predominant with an average annual rainfall of 567 mm and average temperatures around 10°C. The soil is characterized by a calcareous sandy to loamy silt (18.3% sand, 57.2% silt and 24.5% clay) at a pH level of 7.4 and is classified as a calcareous Chernozem.

In March 2011 the site was used as an experimental site for a project of the Austrian Institute of Technology. Thus, 16 circular plots (6.5 meter diameter) were established on this agricultural site. In 2011 the plots were subject to different treatments with four replicates per treatment (see table 1). The treatments comprised a control unit (NPK) where a balanced nitrogen (N) -phosphorus (P) -potassium (K) fertilizer was applied at a N-rate of 120 Kg N ha⁻¹. BC1N was treated with the same

amount of fertilizer as the NPK treatment plots. Additionally, biochar at a rate of 24 t ha⁻¹ was incorporated. The final treatment (BC3N) had the same treatment as BC1N, except 72 t biochar ha⁻¹ were applied.

Table 1: Plot treatments

	Biochar (t ha ⁻¹)	Nitrogen fertilizer (kg ha ⁻¹)
NPK (reference soil)	0	120
BC1N (1:1)	24	120
BC3N (1:3)	72	120

Biochar was produced by S.C. Romchar S.R.L. (Harghita, Romania) using a two-hour pyrolysis process at a temperature of 500°C. The feedstock material was 80% beech and 20% other hardwoods resulting in a biochar conformation of 80.3% C, 9.9% O, 1.6% H and 0.4% N. Biochar was incorporated into the soil in 2011 to a depth of 10 cm using a rotary hoe. The arable land has been managed in a business-as-usual setting by a farmer since then. In 2015 the site was transformed into a vineyard with subsequent changes in agricultural practice and ploughed to a depth of 15 cm.

2.2. Soil sampling and experimental design

Soil samples (3kg per treatment) were extracted from the agricultural site on October 23rd, 2015 from the BC1N, BC3N and NPK plots. The upper 10 cm of the top soil was used. The samples were taken from each replica plot to create a composite sample with average water content. Soil samples were stored at 4°C until they were sieved through a 4 mm mesh. 250 g of sieved moist soil was packed into cores (measurement: 7 cm diameter and 8 cm height) and placed in 1 L Kilner-jars which acted as gas tight flow through mesocosms.

N₂O fluxes were measured and the NH₄⁺/NO₃⁻ concentrations in soil were determined. For this matter two different samples were used in order to avoid a bias in N₂O sampling when extracting 2 g soil for NH₄⁺/NO₃⁻ extraction at each time of sampling.

Samples were taken 4 h (T4), 24 h (T24), 48 h (T48), 72 h (T72) and 2 weeks (T504) after the injection of a treatment solution. Six replicates were measured for each time slot. All jars were allocated to a block consisting of three samples each (one NPK, one BC1N and one BC3N sample) randomized within the blocks. The order of the samples at T0 (injection) and T4, T24 was kept the same, but randomized for T48, T72 and T504. This was performed for the N₂O analysis and the NH₄⁺/NO₃⁻ analysis accordingly. After 48 h, the samples were watered 20 hours before further measurements were taken. Therefore, samples were weighed after the initial injection to apply demineralized water according to the losses by overnight evaporation.

A 500 ml solution containing 6.45 g of KNO₃ (¹⁵N enriched at 5.56 atom%) and 1.75 g of NH₄Cl (at natural abundance) was added. This gave us a soil concentration of 50 ppm NO₃-N and 25 ppm NH₄-N. The solution was injected to the soil cores at T0. The solution was equally distributed throughout the soil core with a multi-needle injector. All chemicals were obtained from Sigma Aldrich (AUT).

This procedure was repeated for all batches over two weeks. Measurements were taken of three replicates of each treatment per week. The exact same procedure was followed in both weeks.

2.3. Inorganic N determination

Measurements of inorganic-N were conducted according to Hood Nowotny et al. (2010).

To extract inorganic N, 2 g of the ¹⁵N-labeled soil was extracted after T4, T24, T48 and T72 and shaken with 15 ml of 0.5M K₂SO₄ in polypropylene vessels for 60 minutes. The extract was filtered through a Whatman 42 ashless filter paper. All samples were frozen at -20°C until further analysis.

The extraction was performed at the International Atomic Energy Agency (IAEA - Seibersdorf, AUT). NO₃⁻ and NH₄⁺ concentrations in the extract were determined using colorimetric assays as described below.

Nitrate

The VCl_3 method (according to Hood-Nowotny et al., 2010) was used for NO_3^- determination: 100 μl sample/standard was pipetted into a microtiter plate together with 100 μl acidic VCl_3 , 50 μl Griess Reagent I and 50 μl Griess Reagent II (see figure 4). Samples were incubated for 60 minutes at 37°C . Both, the samples and the standards were then measured in a microtiter plate reader at 540 nm (EnSpire, Perkin Elmer).

Acidic VCl_3 was prepared shortly before use by mixing 1M HCl and 50.9mM VCl_3 (by Sigma-Aldrich). The solution was filtered through Whatman ashless filter paper. Griess Reagent I consisted of 0.77mM N-naphtylethylenediamine dihydrochlorinade. Griess Reagent II was generated by mixing 3M HCl and 10 g l^{-1} sulfanilamide.

Ammonium

For determining the NH_4^+ concentration 100 μl sample/standard were mixed in microtiter plates with 50 μl NH_4^+ Colour Reagent and 20 μl Oxidation Reagent. After 30 minutes of incubation at 21°C it was measured in a microtiter plate reader at 660 nm.

The NH_4^+ Colour Reagent was produced by mixing 170 g l^{-1} Na-salicylat and 1.278 g l^{-1} Na-nitroprusside and diluted in a 1:1:1 ratio with water and 0.3M NaOH. The oxidation reagent is prepared with 1 g l^{-1} dichloroisocyanuric acid.

The standards for both NH_4^+ and NO_3^- determination were prepared in Eppendorfer tubes at an initial concentration of 20 $\mu\text{g N ml}^{-1}$. NO_3^- and NH_4^+ diluted using a 1:8 serial dilution with 0.5M K_2SO_4 . Standards were pipetted into a microtiter plate, similar to the samples, and mixed with the same solutions as needed for NO_3^- and NH_4^+ determination.

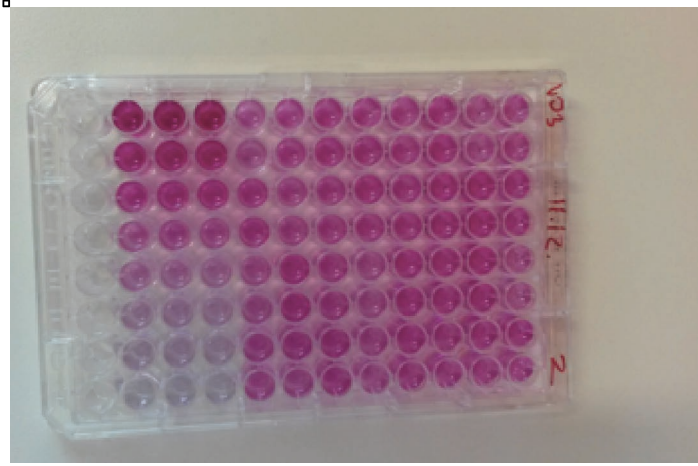


Figure 4. Nitrate determination with the EnSpire microtiter plate reader

2.4. Micro diffusion and isotope ratio mass spectrometry

Isotope analysis was performed with an isotope ratio mass spectrometer (IRMS) at IAEA, Seibersdorf, with samples prepared using micro diffusion (IAEA, 2001).

After analysing the $\text{NH}_4\text{-N}$ and $\text{NO}_3\text{-N}$ concentrations of the soil, appropriate extract volumes (see equation 1) were pipetted into polypropylene vessels.

Equation 1. Actual N- concentration X_{NH_4} for IRMS of ammonium samples

$$X_{\text{NH}_4} = m \frac{A_{\text{xp}} \cdot 8}{A_{\text{HN}}}$$

X_{const} is the amount of the solution needed for the IRMS. A 50 ml solution was used as a constant value for this study. The concentration of $\text{NH}_4\text{-N}$ was based on the absorbance of NH_4^+ concentration generated by the EnSpire microtiter plate reader which was diluted by the factor 8. A similar calculation applies for the NO_3^- determination:

Equation 2. Actual N- concentration X_{NO_3} for IRMS of nitrate samples

$$X_{\text{H}_4} = m \frac{A_{\text{xp}} \cdot 8}{A_{\text{H}_4}}$$

All samples with a volume < 5 ml were diluted with KCl in order to ensure correct measurements with the IRMS. KCl was used instead of K_2SO_4 due to availability issues of chemicals. In the next step, acidified quartz fibre discs were prepared and placed into each vessel. When preparing the discs, Whatman quartz filter paper was cut into discs (diameter= 4 mm) using a paper punch. The discs were placed on Teflon tape. After pipetting 10 μ l $KHSO_4$ onto each disc, the strip was covered by putting another layer of Teflon tape over the discs (figure 5). To create an impervious membrane, the Teflon tapes were pressed together by hand using a round cylindrical vessel with a diameter slightly larger than the quartz fibre disc itself. By sealing the Teflon stripes an acid trap was created for NH_4^+ trapping (Sigman et al., 1997).



Figure 5. Preparation for the Micro Diffusion and IRMS

For NH_4 -N determination 200 mg of magnesium oxide (MgO) was added to the soil extract for diffusing ammonium. This increased the pH to > 8.0 resulting in a release of NH_4 -N from the solution as NH_3 -N. The NH_3 was absorbed by the acidified quartz fibre disc. For NO_3^- measurements, the same procedure was adapted, except 200 mg of Devarda's alloy was added as well. The alloy consists of Al, Cu and Zn and reduces NO_3^- to NH_4^+ which is converted to NH_3^+ . The two important process parameters are temperature and pH as the reduction rate rises with an increase of the two parameters (Sigman et al., 1997). The vessels have to be closed right after the application to avoid losses and have to be shaken briefly.

For quality assurance, standards were produced for KNO_3 (^{15}N enriched) and NH_4Cl used for the injection of soil cores. Furthermore, standards were prepared from K_2SO_4 and KCl used for the soil extraction.

All diffusion samples were stored in a dark chamber at room temperature for three days. In this period the quartz fibre discs absorbed all gaseous NH_3 . After this period, the Teflon membrane was opened and the discs were placed into microtiter plates for drying. The dried discs were put into tin cups and carefully sealed. To analyse ^{15}N enrichment of the N contained in the discs, IRMS was used following the principal of the mass-to-charge-ratio of atoms (Sulzman, 2007).

The IRMS generated output data as % ^{15}N , % ^{15}N XS and $\mu\text{g N}$ of NH_4 and the total values of the $\text{NH}_4 + \text{NO}_3$ mixture. For further statistics, the NO_3 value had to be calculated by the following equation.

Equation 3. NO_3 determination by atomic fraction (Source: IAEA, 2001, adapted after equation 42)

$$a_d = \frac{(a_x - a_m) + d * a_m}{d}$$

am...atom fraction of $^{15}\text{N-NH}_4$

ad... atom fraction of $^{15}\text{N-NO}_3$

ax... ^{15}N -mixture

d... proportion of NH_4

To simplify all further analysis ^{15}N XS data were used instead of the natural abundance one by subtracting the background abundance (0.3663%) from the abundance of ^{15}N . By calculating the ratio between % ^{15}N data of the LGR Isotopic N_2O Analyser and the ^{15}N mixture, the percentages of N_2O from the NO_3 pool could be calculated as well as the percentage of N_2O from pools other than the NO_3 one:

Equation 4: Percentage N_2O from the nitrate pool

$$N_2O_{NO_3} = \left(\frac{\%^{15}\text{N}}{15N_{NH_4+NO_3}} \right) * 100$$

% ^{15}N is a value calculated by the LGR Isotopic N_2O Analyzer. The term $^{15}\text{N}_{\text{NH}_4+\text{NO}_3}$ represents the mixture of the NH_4 and NO_3 concentrations in the solution analysed by the IRMS. The N_2O concentration from pools other than the NO_3 pool is calculated by $100 - \text{N}_2\text{O}_{\text{NO}_3}$.

2.5. N_2O sampling

The N_2O analyses were performed at IAEA (Seibersdorf, AUT) with an Isotopic N_2O Analyzer (Model 914-0027 LGR- Los Gatos Research –California).

The analyser forms a dynamic closed system for determining N_2O emissions. The Isotopic N_2O Analyzer consists of an engine pumping background gas through tubes to the sealed sample. The inlet tube pumps air (at atmospheric conditions) into the jars performing as background N, while the outlet sucks the air out to analyse the difference in atmospheric N and the N emitted from the sample. The Isotopic N_2O Analyzer was operated at an operating temperature of 44.22°C and pressure of 45.02 torr.

When using the Isotopic N_2O Analyzer, each jar was sealed and connected to the analyser via inlet and outlet tubes connected to the lid by 3-way valves to create through flow (figure 6). For the 15 minutes of measurement the jars were placed in a growth chamber (Rubart Aparath GmbH) at 25°C and 65% moisture content. When not measuring the N_2O level, the samples were stored at 22°C .



Figure 6. LGR measurement system for N₂O determination

The N₂O analyser was used at a rate of 0.5 Hz – measuring N₂O levels every 2 seconds. The standard error was reported as average. $\delta^{15}\text{N}$, $\delta^{15}\text{N}_\alpha$, $\delta^{15}\text{N}_\beta$ and $\delta^{18}\text{O}$ were determined for isotope ratio measurements in parts-per-thousand (pp-mil). The isotope ratio of $\delta^{15}\text{N}$ was measured relative to the air-N level in the growth chamber by the equation 5.

Equation 5: Isotope ratio vs. air-Nitrogen (Source: Los Gatos Research, s.a.)

$$\delta^{15}\text{N} = m \left[\frac{\left(\frac{15}{14} \right)_{\text{sample}} / \left(\frac{15}{14} \right)_{\text{air}} - 1 \right] \times 1000$$

Similar to the NO₃/NH₄ determination, samples were measured after 4, 24, 48 and 72 hours as well as after 2 weeks according to a time schedule. One day before the application of the solution, a N₂O baseline was created by measuring soil samples without prior injection. At T4, T24, T48, T72 and T504 measurements were taken every 18 minutes. The first 15 minutes accounted for the actual measurement of the Isotopic N₂O Analyzer followed by a period of three minutes measurement without any input to decrease the N₂O level within the tubes to a baseline level.

2.6. Gross vs. Net Nitrification

Nitrification rates were analysed in two different ways to determine gross nitrification and net nitrification.

Net nitrification rates were calculated by the losses of the NH_4 pool and the NO_3 pool respectively. The slope between the times within each treatment was used to determine the nitrification rate between T4 and T24, T24 and T48 as well as the rate between T48 and T72. This calculation was done for each treatment separately.

The gross nitrification rate was initially calculated using the classical Barraclough method to determine nitrification rates (Mary et al., 1998). This method assumes a positive change of the nitrification rate in the NO_3 pool. In our case, there was a negative rate for the NO_3 pool found. Therefore, this method had to be neglected. Instead, we used an isotopic two-pool-source mixing model (Mary et al., 1998). The gross nitrification rates at each time (T4 to T72) were calculated according to equation 6.

Equation 6: Isotopic two-pool-source mixing model

$$\frac{\Delta \text{NO}_3}{\Delta t} = \frac{(x_{\text{ST0}}/100) * x_{\text{T0}}}{(x_{\text{T1}}/100)}$$

x_{ST0} is the XS value of the isotopic enrichment of NO_3^- . x_{T0} is the concentration of $\text{NO}_3\text{-N}$ in $\mu\text{g N g}^{-1}$ soil at the starting time. x_{T1} is the concentration of $\text{NO}_3\text{-N}$ in $\mu\text{g N g}^{-1}$ soil at the end. For the interval T4 to T24, x_{T0} stands for the measurements at T4 and x_{T1} are the ones at T24. Dividing it by 24 results in the gross nitrification rate per hour. This model does not measure the change in pool size between time intervals, as the Barraclough model suggests, it rather calculates the gross nitrification rate at a certain time.

2.7. Statistical Analysis

The statistical analysis for N₂O flux data was performed by using Minitab (17). Data was found to be heterogeneous and non-normal. A log+1 transformation was used for statistical analysis for passing normality tests.

Measurements were taken in two separate weeks. To determine a potential significant relation between the batches of the two weeks and the treatment of the samples, a two-way-ANOVA was performed. There was no indication that a correlation between the two factors exist. Hence, for further statistics it was assumed that all samples were measured in the same timeframe.

The relation between time (T0 to T504) and treatment was analysed with a Generalized Linear Model as parametric test. Normality of the data was checked with the Turkey test. In order to display the original decay T0 was neglected for the statistical analysis. The normality test was passed in all cases except from the data for N₂O from the NO₃ pool. In this case, a Mood's median test was performed as non-parametric test.

3. Results

We intended to investigate the impact of biochar on the inorganic N status of our soil and the nitrification rates five years after its incorporation. Secondly, we observed how these changes may affect the sources of N₂O emission by using the LGR Isotopic N₂O Analyzer.

This chapter includes the results of the measurements described in the previous chapter. First, the output of the IRMS showing the inorganic N concentrations of NH₄⁺ and NO₃⁻ is described. Furthermore, the data from the LGR Isotopic N₂O Analyzer is presented. Lastly, the analysis of nitrification rates is presented by comparing gross nitrification and net nitrification.

3.1. Inorganic N determination

Table 2 shows the inorganic components of N that were measured and calculated on the basis of the micro-diffusion and IRMS. Moreover, the ^{15}N labelled NO_3^- and NH_4^+ data ($^{15}\text{N-NH}_4 \text{ XS}/^{15}\text{N-NO}_3 \text{ XS}$) was measured. It can be observed that the enriched ^{15}N was not only found in the NO_3^- samples but also in the NH_4^+ samples.

Table 2. Inorganic N concentrations in soils and isotopic signature determined from K_2SO_4 soil extracts.

Time	Treatment		$\text{NH}_4 \mu\text{N/g soil}$	$\text{NO}_3 \mu\text{g/g soil}$	$^{15}\text{N-NH}_4 \text{ XS}$	$^{15}\text{N-NO}_3 \text{ XS}$
T0	NPK	Average	5.09	5.19		
		SD	0.26	0.40		
	BC1N	Average	4.85	6.29		
		SD	0.88	2.28		
	BC3N	Average	5.02	5.25		
		SD	0.43	0.70		
T4	NPK	Average	47.66	88.68	0.02	2.98
		SD	14.99	40.46	0.03	0.34
	BC1N	Average	59.40	128.79	0.03	2.83
		SD	10.98	87.55	0.03	0.85
	BC3N	Average	54.17	117.34	0.02	2.69
		SD	7.21	36.38	0.02	1.05
T24	NPK	Average	38.93	108.95	0.01	3.02
		SD	5.81	64.78	0.01	0.90
	BC1N	Average	43.31	92.25	0.01	3.33
		SD	10.77	18.78	0.01	0.33
	BC3N	Average	36.20	116.29	0.01	3.61
		SD	9.28	80.32	0.00	0.13
T48	NPK	Average	29.34	94.55	0.01	2.59
		SD	3.53	19.82	0.01	0.67
	BC1N	Average	27.43	87.64	0.01	2.71
		SD	2.61	14.25	0.02	0.65
	BC3N	Average	30.83	90.73	0.01	2.49
		SD	3.83	22.83	0.02	0.72
T72	NPK	Average	23.89	86.20	0.02	3.40
		SD	1.04	18.40	0.01	0.10
	BC1N	Average	25.63	83.79	0.02	3.33
		SD	2.08	9.30	0.01	0.19
	BC3N	Average	26.45	92.80	0.03	3.37
		SD	4.38	6.80	0.02	0.21

T504	NPK	Average	27.91	84.78	0.00	2.75
		SD	3.18	13.36	0.00	0.43
	BC1N	Average	31.54	76.85	0.00	2.65
		SD	6.50	10.07	0.00	0.16
	BC3N	Average	27.20	98.87	0.00	3.01
		SD	2.47	11.54	0.00	0.12

In table 2 it can be observed that the measured NH_4 data at T0 is far lower in all treatments than the equivalent measurements during the other time slots. At T4 there can be observed a peak in all treatment plots occurring due to the prior injection of the ammonium-nitrate solution. Figure 7 shows the changes in soil NH_4^+ versus time. The figure shows the additional NH_4^+ that was added at T0 resulted in a peak at T4, following the expected decay until T504. There is a strong decay in NH_4^+ concentration until T48 but an almost linear relation between T48 and T504. There was no significant treatment effect between treatments NPK, BC1N and BC3N. The statistical analysis however showed significant time effects for the decay of the NH_4^+ concentration in the samples.

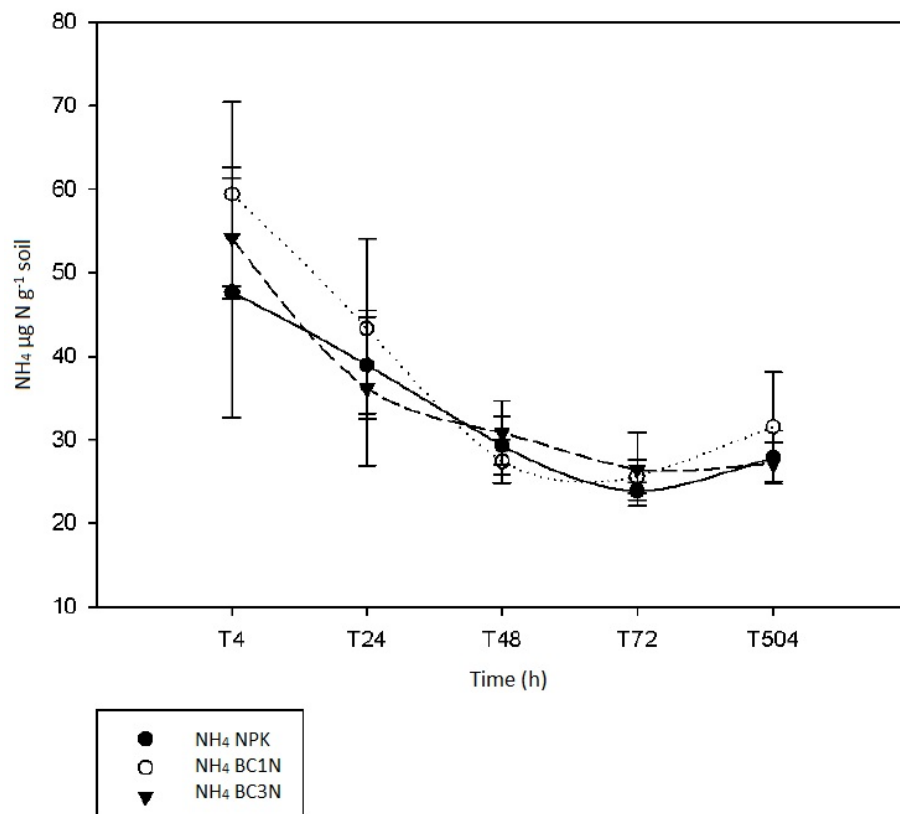


Figure 7. Concentration of ammonium in soils plotted against time

For the inorganic NO_3^- concentrations there was no significant treatment effect found (figure 8). Other than the NH_4^+ concentration, NO_3^- concentrations did not show any significant correlation between times T4 to T504. After the initial increase in NO_3^- concentration due to the added solution at T0 there cannot be observed a clear decay as for the NH_4^+ concentration. Although in both cases it seems like the NPK treatment has lower NO_3^- and NH_4^+ concentrations at T4, no statistical significance could be found. Other than expected it seems like the NO_3^- was added at T0 could not be fully traced at T4 and does not show a symptomatic decay.

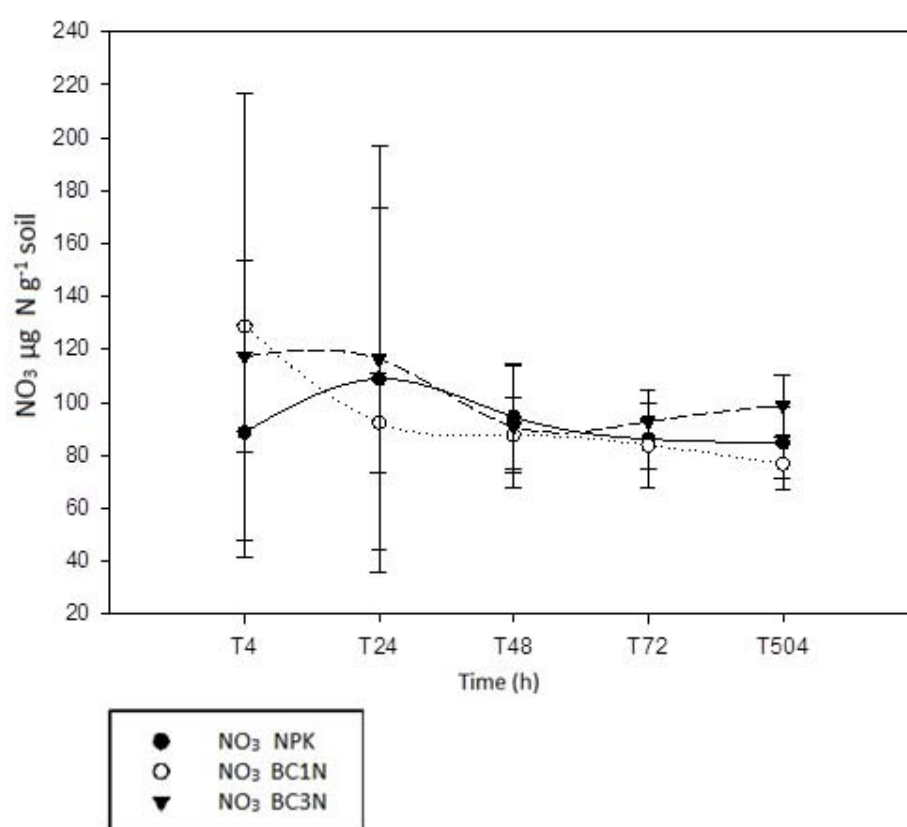


Figure 8. Concentration of nitrate in soils plotted against time

3.2. N_2O gaseous analysis

The LGR Isotopic N_2O Analyser delivered results for ^{15}N -nitrogen, $\delta^{15}\text{N } \alpha$, $\delta^{15}\text{N } \beta$, $\delta^{17}\text{O}$, and $\delta^{18}\text{O}$ in N_2O . For this study, an Excel macro was developed to transform the output data into the needed variables $\text{kg ha}^{-1}\text{a}^{-1}$, N_2O -flux and $\% ^{15}\text{N}$.

Table 3 presents the results for the gaseous emissions from the LGR Isotopic N₂O Analyzer. The data is represented in the figures 10 and 11.

Table 3. Gas emissions from N₂O analysis

Time	Treatment		N ₂ O-flux/ h	% N ₂ O (NO ₃ pool)	% N ₂ O (other pools)	% ¹⁵ N
T0	NPK	Average	0.01			0.42
		SD	0.00			0.21
	BC1N	Average	0.00			0.35
		SD	0.01			0.04
	BC3N	Average	0.01			0.40
		SD	0.01			0.08
T4	NPK	Average	0.05	31.51	68.49	1.05
		SD	0.01	3.55	3.55	0.05
	BC1N	Average	0.05	32.97	67.03	0.97
		SD	0.01	13.00	13.00	0.06
	BC3N	Average	0.05	36.57	63.43	0.97
		SD	0.01	16.57	16.57	0.02
T24	NPK	Average	0.10	34.96	65.04	1.06
		SD	0.01	17.07	17.07	0.02
	BC1N	Average	0.10	26.69	73.31	0.98
		SD	0.02	2.44	2.44	0.02
	BC3N	Average	0.11	41.65	58.35	1.04
		SD	0.02	37.10	37.10	0.05
T48	NPK	Average	0.10	37.82	62.18	1.08
		SD	0.01	7.55	7.55	0.02
	BC1N	Average	0.10	33.94	66.06	1.00
		SD	0.01	8.01	8.01	0.04
	BC3N	Average	0.11	40.00	60.00	1.08
		SD	0.01	10.60	10.60	0.07
T72	NPK	Average	0.06	29.75	70.25	1.12
		SD	0.00	2.73	2.73	0.09
	BC1N	Average	0.07	28.91	71.09	1.02
		SD	0.01	3.69	3.69	0.02
	BC3N	Average	0.07	29.56	70.44	1.10
		SD	0.01	1.33	1.33	0.07
T504	NPK	Average	0.01	35.43	64.57	
		SD	0.01	29.01	29.01	
	BC1N	Average	0.01	36.26	63.74	
		SD	0.00	19.94	19.94	
	BC3N	Average	0.01	32.16	67.84	
		SD	0.00	32.77	32.77	

According to the flux data (ppm/h) there was an increase in N₂O flux from T4 to T24. While the rates were approximately constant between T24 and T48 in all treatments accordingly, the flux decreased between T48 and T504 back to the initial flux level of T0 (figure 9). The statistical analysis showed no significance treatment effects.

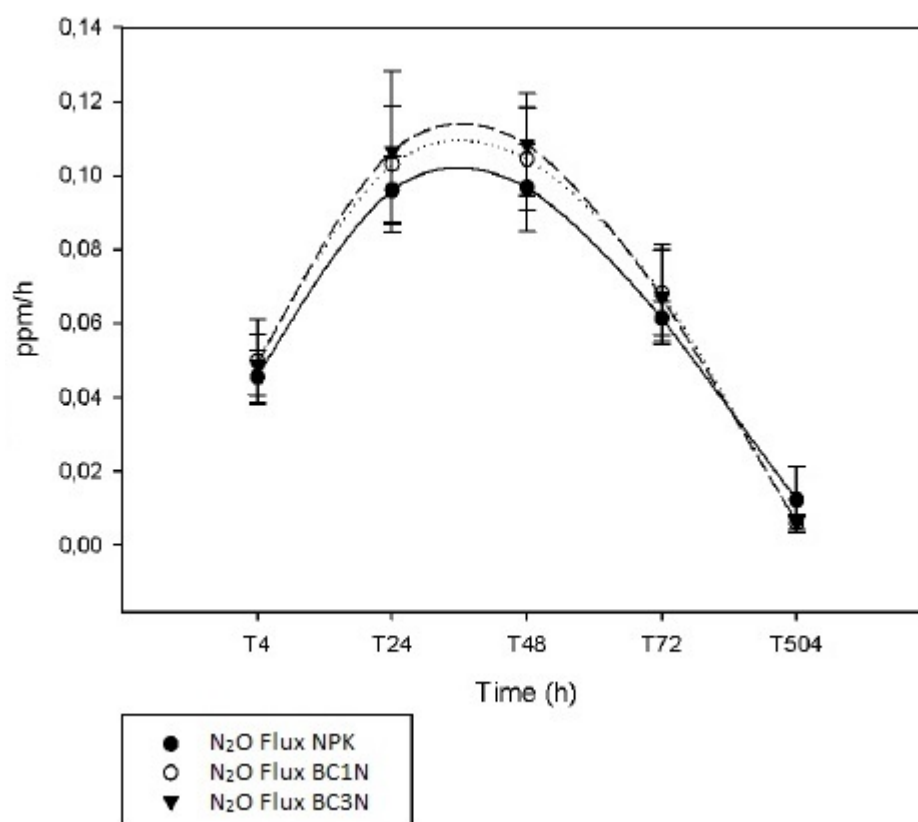


Figure 9. N₂O flux data

The proportion of N₂O-N to different pools shows a negative correlation between N₂O from nitrate pool and from other pools (figure 10). In both cases there is no statistical significance between treatments. The same appears for the time effect were no correlation can be observed. It can be stated, that the level of N₂O derived from the NO₃⁻ pool is half as high as N₂O from all other pools. The fairly linear trend of NO₃⁻ concentration as shown in figure 8 can be observed for the N₂O emissions from the NO₃⁻ pool.

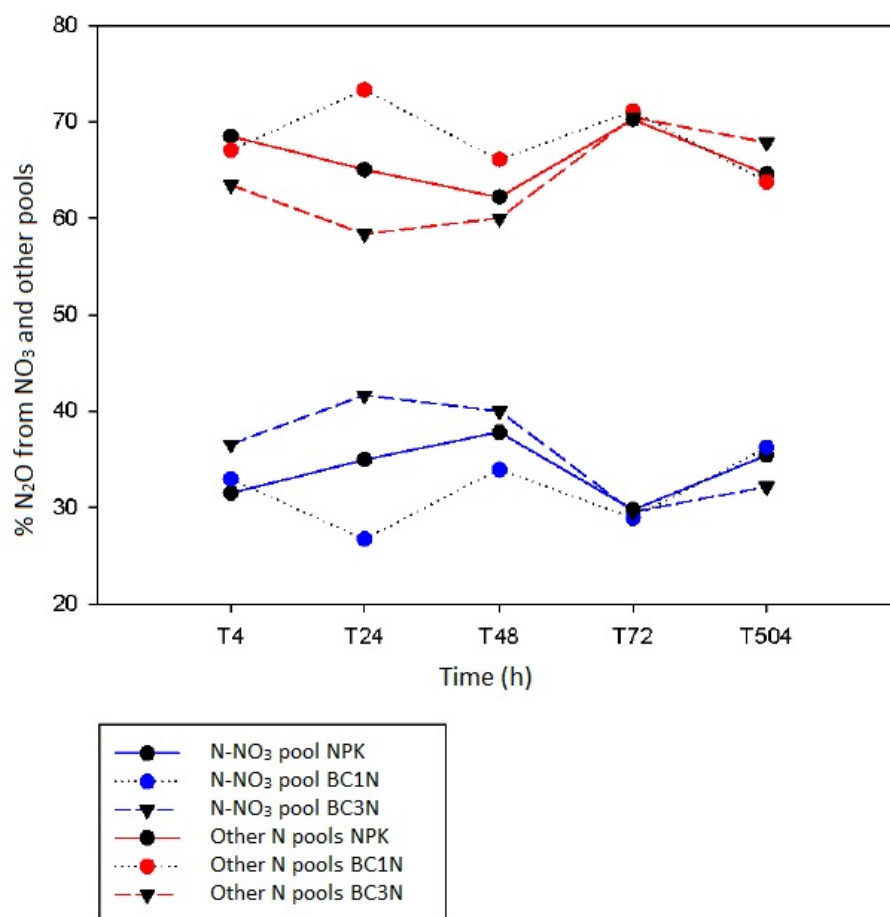


Figure 10. Proportion of N₂O emissions from NO₃ and all other pools

3.3. Nitrification Rates

Nitrification rates were calculated for gross nitrification and net nitrification separately. Net nitrification was calculated for the time intervals T4-T24, T24-T48 and T48-T72 for the NH₄⁺ pool and the NO₃⁻ pool.

Table 4. Net nitrification rates

Time Intervals	Net Nitrification loss of NH ₄ from the NH ₄ pool [NH ₄ µg N g ⁻¹ soil per h]			Net Nitrification increase in NO ₃ concentration [NO ₃ µg N g ⁻¹ soil per h]		
	NPK	BC1N	BC3N	NPK	BC1N	BC3N
T4-T24	0.437	0.805	0.899	-1.013	0.078	0.052
T24-T48	0.400	0.662	0.224	0.600	0.192	1.065
T48-T72	0.227	0.075	0.182	0.348	0.161	-0.086

The net nitrification rate calculated by ΔNH_4 has a clear negative decay of the slope in all treatments between each time interval. The net nitrification rate calculated by ΔNO_3 in contrast indicates that all treatments show a positive slope between T4 and T24 but a negative one between T48 and T72 (figure 11). We would have expected a decrease of the nitrification rates of NO_3 . Therefore, it seems like the NH_4 data is more reliable regarding its significance for net nitrification rates.

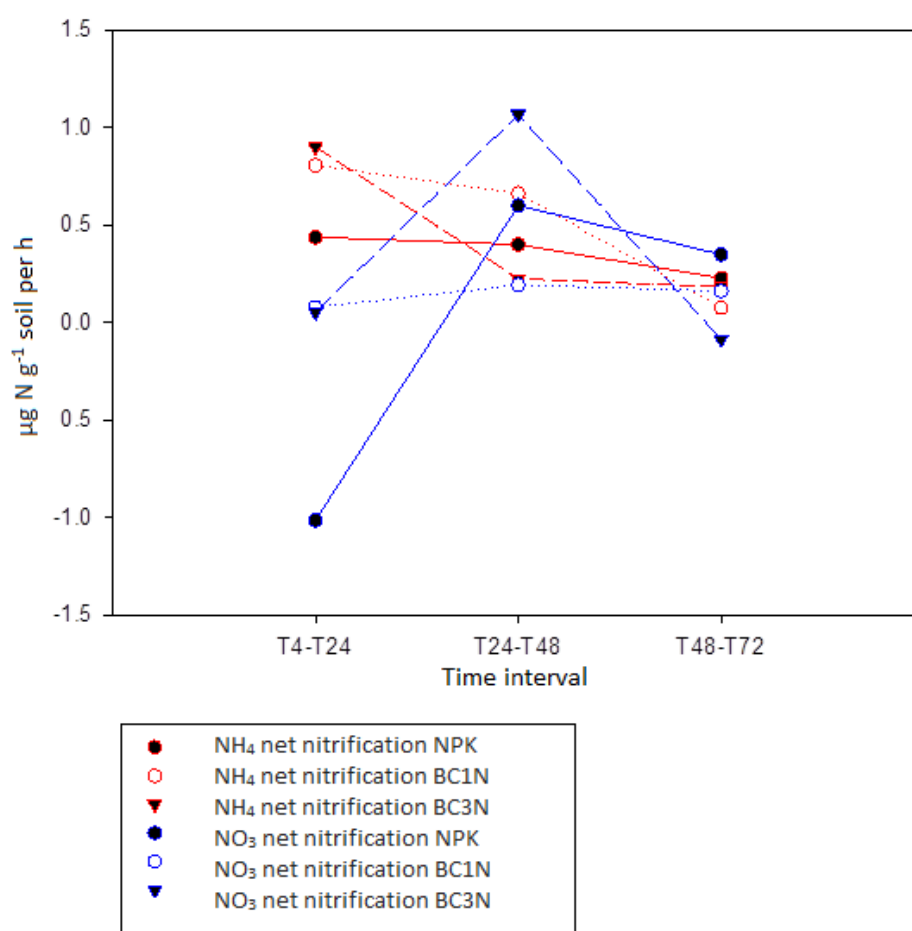


Figure 11. Net nitrification rates of NO_3 and NH_4 sources

The gross nitrification rates were calculated at times T4, T24, T48 and T72 for each treatment (table 5, figure 12). It can be observed, that there are two peaks in all treatments at T24 and T72. There is a drop in all three treatments at time T48. The differences between treatments are not significant from T24 to T72.

Table 5. Gross nitrification rates

Gross Nitrification [NO₃ µg N g⁻¹ soil per h]			
Time	NPK	BC1N	BC3N
T4	2.78	4.38	3.50
SD	0.24	0.81	0.38
T24	4.70	4.77	5.06
SD	0.45	0.27	1.11
T48	3.08	2.93	2.81
SD	0.58	0.32	0.24
T72	4.46	4.38	4.28
SD	0.36	0.20	0.18

As the NH₄⁺ data (figure 7) was found to be fairly linear between T48 and T504 with only very small changes in the NH₄ pool size which might suggest that the rate of nitrification went close to zero. The gross nitrification rates can be best illustrated using the times T4, T24 and T48. After the initial increase in gross nitrification there is a rapid decay between T24 and T48 to a level lower than the initial level at T4 (figure 12). The three treatments in T4 are different from each other with the NPK treatment having the lowest gross nitrification rate and the BC1N treatment the highest rates. However, there cannot be seen a treatment effect at T24 and T48.

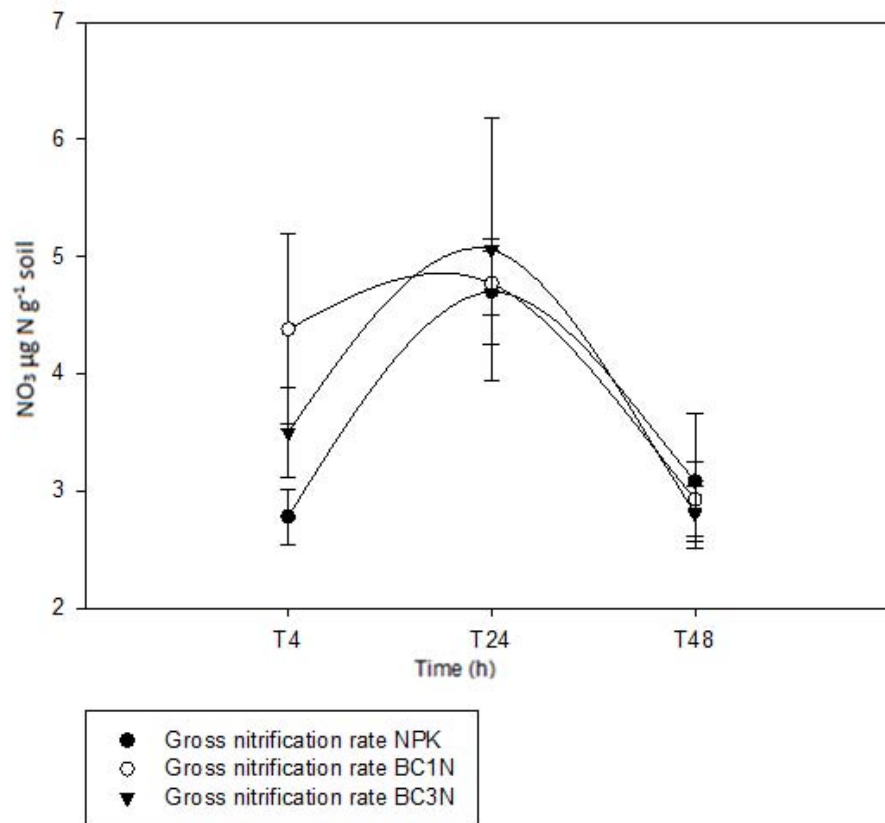


Figure 12. Gross nitrification rates per hour

4. Discussion

The objective of this thesis was to determine the mechanisms behind N₂O emissions from biochar amended soil. Nitrification and denitrification were analysed and the pathways of nitrifier denitrification, ammonia oxidation and heterotrophic denitrification were observed. Furthermore, the effect of biochar on soil five years after its application in 2011 was studied.

In the next paragraphs, the results are discussed for each experiment. Furthermore, an explanation of the effects of biochar in the single experiments is discussed.

4.1. Inorganic N determination

The rather high standard deviations in some replicates might indicate N₂O hot-spots in the samples. This affects the significance of the measurements. However, we could observe several abnormalities that can be traced back to different mechanisms. The

^{15}N labelled nitrate and ammonium data ($^{15}\text{N}\text{-NH}_4$ XS/ $^{15}\text{N}\text{-NO}_3$ XS) was supposed to show a clear enrichment of NO_3^- . However, in these samples there were also small traces of ^{15}N enriched NH_4^+ found. We could not account for the losses in the NO_3^- concentration. There can be several reasons for this. It could have occurred due to a crossover in the sample preparation during the storage of samples in the desiccator. However, acid traps were included in the system and a number of blanks were integrated in the experiment to assess this matter. Another possible explanation is that ^{15}N enriched NH_4^+ was found due to dissimilatory NO_3^- reduction to NH_4^+ (DNRA). This might suggest that there could be other processes in place than the ones assumed in this thesis. These might be losses to denitrification, mineralization or N-leaching or other microbiological activities. RNA analysis via QPCR might help understanding the mechanisms behind this rather unexpected phenomenon.

4.2. N_2O gaseous analysis

The actual percentage of N from various pools was measured and differentiated by the NO_3^- pool and all other pools. Figure 11 clearly shows that the amount of N_2O derived from the NH_4^+ and other pools is much higher than N_2O emissions from the NO_3^- pool. Hu et al. (2015) state that nitrification in ^{15}N enrichment studies is derived from $\text{NH}_4\text{-N}$, while denitrification can be traced back to $\text{NO}_3\text{-N}$. Hence it can be stated that N_2O emissions are only partly derived from denitrification in our study. However, the major part of emissions comes from other mechanisms than denitrification.

This is contradicting to several other studies. Case et al. (2015) for example, observed that denitrification accounts for the majority of N_2O emissions from arable soil. In their case, biochar significantly decreased N_2O emissions. Denitrification rates in biochar amended soil accounted up to 95% compared to 85% in the reference soil without biochar. The proportion of the denitrification, nitrification and nitrifier denitrification were equal in biochar treated and untreated soil. This significant influence of biochar can clearly not be observed in our study.

Due to the results presented in table 2 it becomes obvious, that N_2O emissions derived from denitrification only play a minor role as ^{15}N from $\text{NO}_3\text{-N}$ is very limited. In this study ammonia oxidation and nitrifier denitrification accounted for around 70 % of all emissions. However, Hu et al. (2015) observed that it is not feasible to

differentiate between ammonia oxidation and nitrifier denitrification with this technique alone. This might be quantified by a dual labelling technique as developed by Wrage et al. (2005), where ^{18}O of the H_2O is labelled and measured accordingly however there have also been problems with the assumptions made in these techniques due to exchange of ^{18}O .

Other mechanisms that might affect the pool size distribution might include nitrification, mineralization and leaching. With the applied techniques it is though not possible to differentiate between those other sources.

4.3. Nitrification rates

The study conducted in 2011 and 2012 by Prommer et al. (2014) on the same experimental site showed that gross nitrification rates significantly increased after biochar incorporation.

The net nitrification rate is the increase in the NO_3 pool and the losses of the NH_4 pool over time. It was expected that nitrification would lead to an increase in the NO_3 pool size indicating that nitrification was occurring. However, in our case, we see a clear negative change in the NO_3 pool, which suggests a loss mechanism of NO_3^- . We suspect this loss to be denitrification and NO_3^- resulting directly in N_2 emissions. We see a dilution of the isotope label in the NO_3 pool suggesting that nitrification is occurring. The loss of NH_4^+ from the NH_4 pool again suggests active nitrification. However, we see no concurrent increase in the NO_3^- concentration of the NO_3 pool suggesting that NO_3^- is lost from the system. We suspect this is in the form of N_2 but we have not measured it. Another explanation could be the uptake of NO_3^- by the microbial biomass however microbial uptake of NO_3^- has been rarely reported. Denitrification over all times only occurs at the BC3N treatment. The results indicate, that in the two other treatments (NPK and BC1N) nitrification appears between T4 and T24. This however changes to denitrification losses between T24 and T72.

The classical Barraclough method (Mary et al., 1998) relies on the positive change in the NO_3 pool size. As there is a high denitrification loss, this method is not feasible for this study. Therefore, we developed a new model according to the isotopic two-pool-source mixing model to calculate the gross nitrification.

When comparing the net nitrification with gross nitrification, it shows that gross nitrification rates are higher than net nitrification rates. This might be a result of NH_4^+ being lost to the NO_3^- pool. The high dilution of the organic matter might be directly adding to the NO_3^- pool. This suggests that there is heterotrophic nitrification happening.

4.4. Biochar vs. non-biochar treatment

The statistical analysis did not show any significant difference between the two biochar treatments and the non-biochar treatment.

In a prior study by Prommer et al. (2014) there was no significant effect of biochar treatment found on NH_4 consumption ($p=0.383$). However, the effect on NO_3 was significant ($p=0.001$). Similar to the NH_4 results of Prommer et al. (2014), there was no significant effect detected in this experiment. However, there was also no significant difference between the three treatments for NO_3 and all other measured parameters. Table 6 shows the treatment effect of the measurements according to their p-values of the generated General Linearized Model. The reason for the missing correlation might be that biochar loses its capacity over time. In this study, biochar was added five years prior to the experiment. As there is a very limited amount of long-term studies on biochar, there is no comparison to other studies possible. It shows though, that on the arable field we extracted our soil from, no positive effects of biochar on the N-cycle can be found on a long term basis.

Table 6. Probability of treatment effects

Measurements				
	NH_4	NO_3	ppm/h	$\text{Kg ha}^{-1}\text{a}^{-1}$
p	0.19	0.45	0.07	0.27

5. Conclusion and Outlook

In this study, there was no significant effect of the different biochar treatments found on N_2O production of the arable soil. Although the biochar particles were clearly

visible in the treated soil, it can be resumed that five years after biochar application on this specific treatment area, no effect of biochar can be found. In some cases, treatments showed outliers that might be accounted for hot-spots in the soil. There might also be a high dependability on site specific conditions as well as the predominant climate, soil classification, biochar feedstock and biochar production parameters. Therefore, it has to be noted that these findings are specific to this agricultural site and the mechanisms of N₂O production might be different under changing conditions. Concluding, the first hypothesis we proposed *Adding biochar results in a shift of N₂O production from heterotrophic nitrification to nitrifier-denitrification* could not be verified by our research results. There was no significant effect of biochar incorporation found on N₂O emissions in our treated plots five years after biochar was incorporated into the soil.

We found that N₂O emissions are only partly derived from denitrification in our study. However, most emissions originate in mechanisms other than denitrification. Hereby, ammonia oxidation and nitrifier denitrification accounted for around 70 % of all emissions. The second hypothesis *N₂O emissions are derived from ammonia oxidation rather than from nitrifier denitrification* could not be answered by the methods used in our study. Therefore, we propose looking into using methods such as the dual labelling method as proposed by Wrage et al. (2005) for further research efforts.

Future efforts in the field of biochar related N₂O emissions have to be taken in future studies:

- **Field studies vs. laboratory studies:** After determining the microbial matters in a laboratory study on disturbed samples, further effort should focus on on-site measurements at the field site, working with undisturbed soil.
- **Evaluation of soil physical parameter:** Nitrification and denitrification is said to depend highly on moisture soil content and temperature. Especially for evaluating the soil moisture content, soil physical parameters have to be taken into account when conducting studies on the biochemical mechanisms behind N₂O emissions.
- **Adapted methods:** A dual labelling approach as suggested by Wrage et al. (2005) should be adapted to differentiate between the sources of nitrification.

- **Further analysis:** Further studies have to observe the interaction of microbiological communities via RNA and DNA analysis on nitrification and denitrification processes. Furthermore, it is essential to assess similar studies under a holistic experimental setup where physical, chemical and microbiological parameters are extensively cross-referenced.

6. References

Abel, S., Peters, A., Trinks, S., Schonsky, H., Facklam, M., and Wessolek, G. (2013). Impact of biochar and hydrochar addition on water retention and water repellency of sandy soil. *Geoderma*, 202-203, pp. 183–191. doi:10.1016/j.geoderma.2013.03.003

Baggs, E.M. (2008). A review of stable isotope techniques for N₂O source partitioning in soils: recent progress, remaining challenges and future considerations. *Rapid Commun. Mass Spectrom.*, 22, pp. 1664–1672.

Barnes, R. T., Gallagher, M. E., Masiello, C. A., Liu, Z., and Dugan, B. (2014). Biochar-induced changes in soil hydraulic conductivity and dissolved nutrient fluxes constrained by laboratory experiments. *PLoS ONE*, 9(9). doi:10.1371/journal.pone.0108340

Bridgewater, A.V. and Peacocke, G.V.C. (2000). Fast pyrolysis processes for biomass. *Renewable and Sustainable Energy Reviews*, 4, pp.1-73.

Brown, R., Del Campo, B., Boateng, A.A., Garcia-Perez, M. and Masek, O. (2015). Fundamentals of biochar production. In: Lehmann, J. and Joseph, S., *Biochar for Environmental Management*, UK, USA: Routledge, pp. 39-62.

Butterbach-Bahl, K., Baggs, E.M., Dannenmann, M., Kiese, R., Zechmeister-Boltenstern, S. (2013). Nitrous oxide emissions from soils: how well do we understand the processes and their controls? *Philosophical transactions of the Royal Society of London. Series B, Biological sciences*, 368 (1621), s.p.

Case, S.D.C. et al., (2015). Biochar suppresses N₂O emissions while maintaining N availability in a sandy loam soil. *Soil Biology and Biochemistry*, 81 (2), pp.178–185.

Available at: <http://dx.doi.org/10.1016/j.soilbio.2014.11.012>.

Chan, K.Y., Van Zwieten, L., Meszaros, I., Downie, A. and Joseph, S. (2008). Using poultry litter biochars as soil amendments. *Australian Journal of Soil Research*, 46, pp. 437-444.

Chia, C.H., Downie, A. and Munroe, P. (2015). Characteristics of biochar: physical and structural properties. In: Lehmann, J. and Joseph, S., *Biochar for Environmental Management*, UK, USA: Routledge, pp. 89-110.

Clough, T., Condrón, L., Kammann, C., and Müller, C. (2013). A Review of Biochar and Soil Nitrogen Dynamics. *Agronomy*, 3(2), pp. 275–293. doi:10.3390/agronomy3020275

Cornelissen, G., Martinsen, V., Shitumbanuma, V., Alling, V., Breedveld, G., Rutherford, D., Sparrevik, M., Hale, S., Obia, A. and Mulder, J. (2013) Biochar effect on maize yield and soil characteristics in five conservation farming sites in Zambia, *Agronomy*, 3, pp. 256– 274.

Dalal, R., Wang, W., Robertson, G.P. and Parton, W. (2003) Nitrous oxide emission from Australian agricultural lands and mitigation options: a review. *Australian Journal of Soil Research*, 41, pp. 165-195.

Forster, P., Ramaswamy, V., Artaxo, P., Bernsten, T., Betts, R., Fahey, D.W., Myhre, G., Nganga, J., Prinn, R., Raga, G., Schulz, M. and Van Dorland, R. (2007). Changes in atmospheric constituents and radiative forcing. In: *Climate Change 2007: the Physical Science basis. Contribution of Working Group I to the Fourth Assessment Report of the Intergovernmental Panel on Climate Change*. Cambridge: Cambridge University Press, pp. 129-234.

Gray, M., Johnson, M. G., Dragila, M. I., and Kleber, M. (2014). Water uptake in biochars: The roles of porosity and hydrophobicity. *Biomass and Bioenergy*, 61, pp. 196–205. doi:10.1016/j.biombioe.2013.12.010

Harter, J., Krause, H.M., Schuettler, S., Ruser, R., Fromme, M., Scholten, T., Kappler, A. and Behrens, S. (2014). Linking N₂O emissions from biochar-amended soil to the structure and function of the N-cycling microbial community. *The International*

Society for Microbial Ecology Journal, 8, pp. 660-674.

Herath, H. M. S. K., Camps-Arbestain, M., and Hedley, M. (2013). Effect of biochar on soil physical properties in two contrasting soils: An Alfisol and an Andisol. *Geoderma*, 209-210, pp. 188–197. doi:10.1016/j.geoderma.2013.06.016

Hirsch, P.R. and Mauchline, T.H. (2015). The Importance of the Microbial N Cycle in Soil for Crop Plant Nutrition, London: Elsevier Ltd. Available at: <http://dx.doi.org/10.1016/bs.aambs.2015.09.001>.

Hood-Nowotny, R., Hinko-Najera Umana, N., Inselbacher, E., Oswald-Lachouani, P. and Wanek, W. (2010). Alternative Methods for Measuring Inorganic, Organic, and Total Dissolved Nitrogen in Soil. *Soil Science Society of America*, 74, pp. 1018-1027.

Hu, H.W., Chen, D., He, J.Z. (2015). Microbial regulation of terrestrial nitrous oxide formation: understanding the biological pathways for prediction of emission rates. *FEMS Microbiological Review*, 39 (5), pp. 729-749.

IAEA (2001). Use of Isotope and Radiation Methods in Soil and Water Management and Crop Nutrition – Manual. Training Course Series 14. Vienna: FAO/IAEA Agriculture and Biotechnology Laboratory.

IPCC (2013). Climate Change 2013: the physical science basis. Contribution of the Working Group I to the Fifth Assessment Report of the Intergovernmental Panel on Climate Change. Cambridge: Cambridge University Press, p. 1535.

Jankowska, H., Swiatkowski, A. and Choma, J. (1991). Active Carbon. New York: Ellis Horwood.

Keiluweit, M., Mico, P.S., Johnson, M. and Kleber, M. (2010). Dynamic molecular structure of plant biomass-derived black carbon (biochar). *Environmental Science and Technology*, 44, pp. 1247-1253.

Kinney, T. J., Masiello, C. A., Dugan, B., Hockaday, W. C., Dean, M. R., Zygourakis, K., and Barnes, R. T. (2012). Hydrologic properties of biochars produced at different temperatures. *Biomass and Bioenergy*, 41, pp. 34–43.

Kool, D.M. et al. (2010). Nitrifier denitrification can be a source of N₂O from soil: A

revised approach to the dual-isotope labelling method. *European Journal of Soil Science*, 61 (5), pp.759–772.

Laird, D.A., Fleming, P., Davis, D.D., Horton, R., Wang, B. and Karlen, D.L. (2010). Impact of biochar amendments on the quality of a typical Midwestern agricultural soil. *Geoderma*, 158, pp. 443-449.

Lim, T. J., Spokas, K. A., Feyereisen, G., and Novak, J. M. (2016). Predicting the impact of biochar additions on soil hydraulic properties. *Chemosphere*, 142, pp. 136–144. doi:10.1016/j.chemosphere.2015.06.069

Los Gatos Research (s.a.) Isotopic N₂O Analyzer User Manual. Document No. 914-U027. CA: LGR.

Lua, A.C., Yang, T. and Guo, J. (2004). Effects of pyrolysis conditions on the properties of activated carbons prepared from pistachio-nut shells. *Journal of Analytical and Applied Pyrolysis*, 72, pp. 279-287.

Mary, B., Recous, S. and Robin, D. (1998). A model for calculating nitrogen fluxes in soil using N-15 tracing. *Soil Biology & Biochemistry*, 30 (14), pp.1963–1979.

Masiello, C., Dugan, B., Brewer, C., Spokas, K., Novak, J., Liu, Z., & Sorrenti, G. (2015). Biochar effects on soil hydrology. In: Lehmann, J. and Joseph, S., *Biochar for Environmental Management*, UK, USA: Routledge, pp. 543-562.

Park, S., Pérez, T., Boering, K.A., Trumbore, S.E., Gil, J., Marquina, S. and Tyler, S.C. (2011) Can N₂O stable isotopes and isotopomers be useful tools to characterize sources and microbial pathways of N₂O production and consumption in tropical soils?. *Global Biogeochemical Cycles*, 25, GB1001. doi:10.1029/2009GB003615.

Prommer, J. Wanek, W., Hofhansl, F., Trojan, D., Offre, P., Urich, T., Schleper, C., Sassmann, S., Kitzler, B., Soja, G., Hood-Nowotny, R. (2014). Biochar decelerates soil organic nitrogen cycling but stimulates soil nitrification in a temperate arable field trial. *PLoS ONE*, 9 (1).

Quin, P.R., Cowie, A.L., Flavel, R.J., Macdonald, L.M., Morris, S.G., Singh, B.P., Young, I.M. and Van Zwieten, L. (2014). Oil mallee biochar improves soil structural

properties-a study with y-ray micro-CT. *Agriculture Ecosystems Environment*, 191, pp. 142-149.

Ravishankara, A.R., Daniel, J.S. and Portmann, R.W. (2009). Nitrous Oxide (N₂O): The dominant ozone-depleting substance emitted in the 21st century. *Science*, 326, pp. 123-125.

Robertson, G.P. and Groffman, P.M. (2007). Nitrogen Transformation. In: Paul, E., *Soil Microbiology, Ecology and Biochemistry*, 3rd ed. Burlington: Academic Press, pp. 341-362.

Robertson, G.P. and Groffman, P.M. (2015). Nitrogen Transformations. In: Paul, E., *Soil Microbiology, Ecology and Biochemistry*, 4th ed. Burlington: Academic Press, pp. 421-446.

Sielhorst, A. (2014). Nitrous oxide emissions from arable soils – effects of long-term tillage and identification of production and consumption processes using stable isotope approaches. Doctoral dissertation. Georg-August-Universität Göttingen.

Sigman, D.M., Altabet, M.A., Michener, R., McCorkle, D.C., Fry, B. and Holmes, R.M. (1997). Natural abundance-level measurement of the nitrogen isotopic composition of oceanic nitrate: an adaptation of the ammonia diffusion method. *Marine Chemistry*, 57, pp. 227-242.

Snider, D.M., Schiff, S.L. and Spoelstra, J. (2009). ¹⁵N/¹⁴N and ¹⁸O/¹⁶O stable isotope ratios of nitrous oxide produced during denitrification in temperate forest soils. *Geochimica et Cosmochimica Acta*, 73 (4), pp. 877–888.

Sulzman, E.W. (2007). Stable isotope chemistry and measurement: a primer. In: Michener, R., and Lajtha, K., *Stable Isotopes in Ecology and Environmental Science* (2nd ed.), Oxford: Blackwell Publishing, pp. 1-21.

Van Zwieten, L., Kammann, C., Cayuela, M.L., Singh, B.P., Joseph, S., Kimber, S., Donne, S., Clough, T. and Spokas, K.A. (2015). Biochar effects on nitrous oxide and methane emissions from soil. In: Lehmann, J. and Joseph, S., *Biochar for Environmental Management*, UK, USA: Routledge, pp. 489-520.

Wrage, N., Van Groenigen, J.W., Oenema, O. and Baggs, E.M. (2005). A novel dual-isotope labelling method for distinguishing between soil sources of N₂O. *Rapid Communications in Mass Spectrometry*, 19 (22), pp. 3298–3306.